Supporting Information

Techno-economic Assessment of Optimised Vacuum Swing Adsorption for Post-Combustion CO_2 Capture from Steam-Methane Reformer Flue Gas

Sai Gokul Subraveti[1], Simon Roussanaly[2,*], Rahul Anantharaman[2], Luca Riboldi[2], and Arvind Rajendran[1,*]

[1]*Department of Chemical and Materials Engineering, University of Alberta, 12th floor, Donadeo Innovation Centre for Engineering (ICE), 9211-116 Street, Edmonton, Alberta T6G1H9, Canada*

[2]*SINTEF Energy Research, NO-7465, Trondheim, Norway*

[*]*Corresponding authors. E-mail: Simon.Roussanaly@sintef.no (Simon Roussanaly), arvind.rajendran@ualberta.ca (Arvind Rajendran)*

S1 Baseline MEA-based CO_2 capture

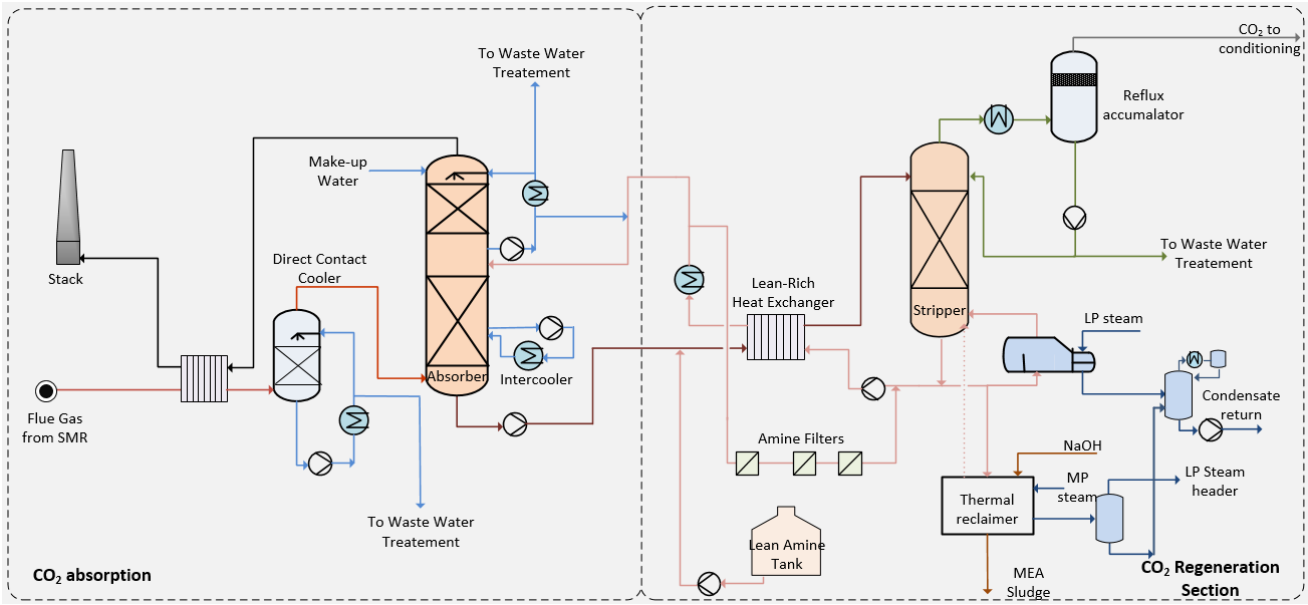

Figure S1: Detailed process flow diagram of the MEA-based CO_2 capture process for the hydrogen production plant with CO_2 capture [1].

Table S1: Key performances of hydrogen production plant without and with MEA-based CCS [2].

Parameter	**Without CCS**	**With CCS**
Natural Gas to feedstock (t h^{-1})	51.66	51.66
Natural Gas to fuel (t h^{-1})	26.59	26.59
Natural Gas LHV (MJ kg^{-1})	46.49	46.49
Total Energy Input (MW)	1010	1010
H_2 to battery limit (t h^{-1})	18.77	18.77
H_2 to battery limit (Nm^3 H_2 h^{-1})	208700	208700
Total energy in H_2 product (MW)	626	626
Gross power output from Steam cycle (MW_e)	123.8	91.6
H_2 plant and co-generation power consumption (MW_e)	-3.5	-3.5
CO_2 capture plant (MW_e)	-	-6.7
CO_2 conditioning plant (MW_e)	-	-18.3
Net Power output (MW_e)	120.3	63.1
Total energy in H_2 product compared Total Energy Input (%)	61.9	61.9
Total energy in H_2 and electricity produced compared Total Energy Input (%)	73.8	68.2
Emissions (kg_{CO_2} Nm^{-3} H_2)	0.994	0.100
Levelised Cost of Hydrogen (c€Nm^{-3} H_2)	12.20	18.07
CO_2 avoidance cost (€/$t_{CO_2,avoided}$)	-	66.6
CO_2 capture cost (€/$t_{CO_2,avoided}$)	-	30.1

S2 Adsorbent Materials

Table S2: Dual-site Langmuir isotherm parameters.

	Zeolite 13X [3]	**UTSA-16** [4]	**IISERP MOF2** [5]
CO_2			
q_{sb} (mol kg^{-1})	3.09	4.08	3.29
q_{sd} (mol kg^{-1})	2.54	1.29	1.89
b_0 (m^3 mol^{-1})	8.65×10^{-7}	2.52×10^{-7}	9.39×10^{-8}
d_0 (m^3 mol^{-1})	2.63×10^{-8}	1.75×10^{-9}	5.23×10^{-7}
ΔU_b (J mol^{-1})	-36641	-32800	-31135
ΔU_d (J mol^{-1})	-35690	-35040	-31135
N_2			
q_{sb} (mol kg^{-1})	3.09	1.33	3.29
q_{sd} (mol kg^{-1})	2.54	1.77	1.89
b_0 (m^3 mol^{-1})	2.69×10^{-6}	9.17×10^{-5}	2.55×10^{-7}
d_0 (m^3 mol^{-1})	2.69×10^{-6}	9.42×10^{-9}	2.55×10^{-7}
ΔU_b (J mol^{-1})	-15710	-7500	-11890
ΔU_d (J mol^{-1})	-15710	-27760	-11890

S3 Technical Modelling of Vacuum Swing Adsorption

S3.1 Model Equations

Component mass balance

$$\frac{\partial y_\mathrm{i}}{\partial t} + \frac{y_\mathrm{i}}{T}\frac{\partial P}{\partial t} - \frac{y_\mathrm{i}}{P}\frac{\partial T}{\partial t} = \frac{T}{P}D_\mathrm{L}\frac{\partial}{\partial z}\left(\frac{P}{T}\frac{\partial y_\mathrm{i}}{\partial z}\right) - \frac{T}{P}\frac{\partial}{\partial z}\left(\frac{y_\mathrm{i}P}{T}v\right) - \frac{RT}{P}\frac{1-\varepsilon}{\varepsilon}\frac{\partial q_\mathrm{i}}{\partial t} \tag{S1}$$

Total mass balance

$$\frac{1}{P}\frac{\partial P}{\partial t} - \frac{1}{T}\frac{\partial T}{\partial t} = -\frac{T}{P}\frac{\partial}{\partial z}\left(\frac{P}{T}v\right) - \frac{RT}{P}\frac{1-\varepsilon}{\varepsilon}\sum_{i=1}^{n_\mathrm{comp}}\frac{\partial q_\mathrm{i}}{\partial t} \tag{S2}$$

Linear driving force model

$$\frac{\partial q_\mathrm{i}}{\partial t} = k_\mathrm{i}(q_\mathrm{i}^* - q_\mathrm{i}) \tag{S3}$$

Mass transfer coefficient (macropore controlled)

$$k_\mathrm{i} = \frac{c_\mathrm{i}}{q_\mathrm{i}^*}\frac{15\varepsilon_\mathrm{p}D_\mathrm{p}}{r_\mathrm{p}^2} \tag{S4}$$

Column energy balance

$$\begin{aligned}\left[\frac{1-\varepsilon}{\varepsilon}\left(\rho_\mathrm{s}C_\mathrm{p,s} + C_\mathrm{p,a}\sum_{i=1}^{n_\mathrm{comp}} q_\mathrm{i}\right)\right]\frac{\partial T}{\partial t} &= \frac{K_\mathrm{z}}{\varepsilon}\frac{\partial^2 T}{\partial z^2} - \frac{C_\mathrm{p,g}}{R}\frac{\partial P}{\partial t} - \frac{C_\mathrm{p,g}}{R}\frac{\partial}{\partial z}(vP) \\ &\quad - \frac{1-\varepsilon}{\varepsilon}C_\mathrm{p,a}T\sum_{i=1}^{n_\mathrm{comp}}\frac{\partial q_\mathrm{i}}{\partial t} + \frac{1-\varepsilon}{\varepsilon}\sum_{i=1}^{n_\mathrm{comp}}\left(\left(-\Delta H\right)\frac{\partial q_\mathrm{i}}{\partial t}\right)\end{aligned} \tag{S5}$$

Pressure drop (Ergun's equation)

$$-\frac{\partial P}{\partial z} = \frac{150}{4}\frac{1}{r_\mathrm{p}^2}\left(\frac{1-\varepsilon}{\varepsilon}\right)^2\mu v + \frac{1.75}{2}\frac{1}{r_\mathrm{p}}\left(\frac{1-\varepsilon}{\varepsilon}\right)\rho|v|v \tag{S6}$$

Ideal gas law

$$c_{\mathrm{i}} = \frac{y_{\mathrm{i}} P}{RT} \tag{S7}$$

Table S3: Boundary conditions for the 4-step VSA cycle.

Step	z=0	z=L
Adsorption	$v\|_{z=0} = v_{\text{feed}}$	$P\|_{\text{z=L}} = P_{\text{H}}$
	$D_{\text{L}} \frac{\partial y_i}{\partial z}\Big\|_{\text{z=0}} = -v\|_{\text{z=0}} \left(y_{i,\text{feed}} - y_i\|_{\text{z=0}}\right)$	$\frac{\partial y_i}{\partial z}\Big\|_{\text{z=L}} = 0$
	$\frac{\partial T}{\partial z}\Big\|_{\text{z=0}} = -\varepsilon\, v\|_{\text{z=0}}\, \rho_{\text{g}} C_{p,\text{g}} (T_{\text{feed}} - T\|_{\text{z=0}})$	$\frac{\partial T}{\partial z}\Big\|_{\text{z=L}} = 0$
Blowdown	$\frac{\partial P}{\partial z}\Big\|_{\text{z=0}} = 0$	$v\|_{\text{z=L}} = v_{\text{vac.pump}}$
	$\frac{\partial y_i}{\partial z}\Big\|_{\text{z=0}} = 0$	$\frac{\partial y_i}{\partial z}\Big\|_{\text{z=L}} = 0$
	$\frac{\partial T}{\partial z}\Big\|_{\text{z=0}} = 0$	$\frac{\partial T}{\partial z}\Big\|_{\text{z=L}} = 0$
Evacuation	$v\|_{\text{z=0}} = v_{\text{vac.pump}}$	$\frac{\partial P}{\partial z}\Big\|_{\text{z=L}} = 0$
	$\frac{\partial y_i}{\partial z}\Big\|_{\text{z=0}} = 0$	$\frac{\partial y_i}{\partial z}\Big\|_{\text{z=L}} = 0$
	$\frac{\partial T}{\partial z}\Big\|_{\text{z=0}} = 0$	$\frac{\partial T}{\partial z}\Big\|_{\text{z=L}} = 0$
Light Product Pressurisation	$\frac{\partial P}{\partial z}\Big\|_{\text{z=0}} = 0$	$v\|_{\text{z=L}} = \frac{v_{\text{ADS}} P_{\text{ADS}}\|_{\text{z=L}}}{P\|_{\text{z=L}}}$
	$\frac{\partial y_i}{\partial z}\Big\|_{\text{z=0}} = 0$	$D_{\text{L}} \frac{\partial y_i}{\partial z}\Big\|_{\text{z=L}} = -v\|_{\text{z=L}} \left(y_{i,\text{feed}} - y_i\|_{\text{z=L}}\right)$
	$\frac{\partial T}{\partial z}\Big\|_{\text{z=0}} = 0$	$\frac{\partial T}{\partial z}\Big\|_{\text{z=L}} = -\varepsilon\, v\|_{\text{z=L}}\, \rho_{\text{g}} C_{\text{pg}} (T_{\text{feed}} - T\|_{\text{z=L}})$

Table S4: VSA simulation parameters.

Parameter	**Value**
Column Properties	
Particle diameter, d_{p} (mm)	1.5
Column void fraction, ϵ_{B} (-)	0.37
Particle void fraction, ϵ_{P} (-)	0.35
Tortuosity, τ (-)	3
Operating Conditions	
Adsorption pressure, P_{H} (bar)	1.02
Inlet feed composition, $y_{\mathrm{CO_2}}/y_{\mathrm{N_2}}$ (-)	0.2/0.8
Inlet feed temperature, T_{feed} (K)	298.15
Physical Properties	
Adsorbent density, ρ_{s} (kg m^{-3})	
Zeolite 13X	1130.0 [3]
UTSA-16	1171.0 [4]
IISERP MOF2	937.7 [5]
Molecular diffusivity, D_{m} (cm^2 s^{-1})	0.16
Fluid viscosity, μ (cP)	0.0172
Specific heat capacity of adsorbent, $C_{\mathrm{p,s}}$ (J kg^{-1} K^{-1})	
Zeolite 13X	1070.0
UTSA-16	1070.0
IISERP MOF2	1070.0
Specific heat capacity of gas phase, $C_{\mathrm{p,g}}$ (J mol^{-1} K^{-1})	30.7
Specific heat capacity of adsorbed phase, $C_{\mathrm{p,a}}$ (J mol^{-1} K^{-1})	30.7
Inside heat transfer coefficient, h_{in} (J m^{-2} K^{-1} s^{-1})	0
Outside heat transfer coefficient, h_{out} (J m^{-2} K^{-1} s^{-1})	0
Effective gas thermal conductivity, K_{z} (J m^{-1} K^{-1} s^{-1})	0.09
Universal gas constant, R (m^3 Pa mol^{-1} K^{-1})	8.314

S3.2 Design of Unit Train

The procedure proposed by Khurana and Farooq [6] was used to determine the column scheduling. Each train comprises minimum number of columns and vacuum pumps necessary for a continuous operation. The minimum number of columns per train was calculated as follows:

$$N = \text{ceiling}\left(\frac{\sum_{i=\text{steps}} t_i}{t_{\text{ADS}}}\right) \tag{S8a}$$

t_i represents the duration of step i in the cycle. The minimum number of blowdown/evacuation vacuum pumps required is given by,

$$N_{\text{V},j} = \text{ceiling}\left(\frac{t_j}{t_{\text{ADS}}}\right) \quad j = \text{blowdown/evacuation} \tag{S8b}$$

If sum of the individual steps in a cycle is not a multiple of the adsorption time, an idle step has to be included after evacuation step so that the bed profiles are least affected [6]. The duration of an idle step was calculated as follows:

$$t_{\text{IDLE}} = N t_{\text{ADS}} - \sum_{i=\text{steps}} t_i \tag{S8c}$$

S3.3 Parallel Trains

A single VSA train might not be sufficient to treat the large volume of flue gas. Hence, several trains of VSA units in parallel are required to capture 90% CO_2 [6, 7]. The number of parallel trains can be calculated as:

$$M = \text{ceiling}\left(\frac{\dot{F}_{\text{flue}}}{\dot{F}_{\text{train}}}\right) \tag{S9}$$

Here $\dot{F}_{\text{flue}}$ is the total flue gas flow rate in kmol h^{-1} and $\dot{F}_{\text{train}}$ is the average molar flow rate of the feed to each train in kmol h^{-1}. It is worth mentioning that the inlet pressure varies over the duration of the adsorption step owing to the constant velocity boundary condition at the feed end. Therefore, the average molar flow rate of feed to each train was calculated based on an integral average of the molar flow rate over the duration of the adsorption step (shown in Eq. S10) and then, used to calculate the number of parallel trains.

$$\dot{F}_{\text{train}} = \frac{1}{t_{\text{ADS}}} \int_0^{t_{\text{ADS}}} \dot{F} dt \tag{S10}$$

S4 Technical Modelling of peripheral units

The implementation of CO_2 capture using VSA technology requires several peripheral units extending from flue gas pre-treatment to CO_2 conditioning. In this section, the technical modeling related to each component unit is discussed below.

Flue Gas Cooling and Drying: The wet flue gas was first cooled to 313.15 K by a direct contact cooler and then dehydrated using a molecular sieve 3Å [8].

Compressors: Single-stage compressors were modeled as an isoentropic compression process. The motor efficiency was assumed to be 100%. The energy consumption was calculated as follows:

$$E_{\mathrm{C}}\ (\mathrm{J_e}) = \frac{1}{\eta_{\mathrm{C}}} \frac{\gamma}{\gamma - 1} \int_{t=0}^{t=t_{\mathrm{ADS}}} QP \left[\left(\frac{P}{P_{\mathrm{ref}}} \right)^{\frac{\gamma-1}{\gamma}} - 1 \right] \mathrm{d}t \tag{S11a}$$

Here η_{C} is the compression efficiency which was assumed to be 80%, γ is the adiabatic constant obtained from a linear regression as a function of CO_2 composition (see Fig. S2), P is the pressure, P_{ref} is the reference pressure of flue gas, t_{ADS} is the adsorption step time and Q is the volumetric flow rate of the feed mixture.

Vacuum Pumps: The energy consumption by a vacuum pump was modeled as an isentropic expansion process as given by,

$$E_{\mathrm{V}}\ (\mathrm{J_e}) = \frac{1}{\eta_{\mathrm{V}}} \frac{\gamma}{\gamma - 1} \int_{t=0}^{t=t_{\mathrm{step}}} QP \left[\left(\frac{P_{\mathrm{atm}}}{P} \right)^{\frac{\gamma-1}{\gamma}} - 1 \right] \mathrm{d}t \tag{S11b}$$

In the above equation, t_{step} is the step duration of blowdown/evacuation step, η_{V} is the vacuum pump efficiency.

Heat Exchangers: Two identical counter-current heat exchangers were considered to cool the dry flue gas after compression to 298.15 K. The design was evaluated based on the cooling duty and the log-mean temperature difference (LMTD) for the counter-current flow. The dry flue gas represents the hot side of the heat exchangers while the cooling water is the cold side. To determine the cooling duty, input and output stream characteristics of the hot dry flue gas were used. While the mass flow rate, input and output temperatures of the dry flue gas were known,

the specific heat capacity was obtained from the National Institute of Standards and Technology (NIST) REFPROP v.9 database [9]. The mass flow rate of the cooling water was then determined by dividing the cooling duty by the heat capacity [9] and an allowable temperature increase of the cooling water. The inlet and outlet temperatures of cooling water were set to 283.15 K and 291.5 K, respectively. The heat exchanger area (A_{EX}) was obtained using,

$$A_{\mathrm{EX}} = \frac{\dot{Q}_{\mathrm{EX}}}{U_{\mathrm{EX}}\mathrm{LMTD}} \tag{S12}$$

where Q_{EX} is the cooling duty (W) and U_{EX} is the overall heat transfer coefficient which is assumed to be around 1000 W m^{-2} K^{-1} for all process heat exchangers [10].

CO_2 Conditioning: The CO_2 after capture undergoes compression from 1 bar, 298.15 K to offshore pipeline transport conditions at 200 bar and 318.15 K. The CO_2 conditioning before pipeline transport was modelled as a four-stage compression system with intercoolers and a pump to deliver the CO_2 at desired pressure in Aspen HYSYS. The readers are referred elsewhere [2] for detailed modeling of CO_2 conditioning.

CO_2 Transport and Storage: The costs of the transport and storage are assessed using the iCCS tool developed by SINTEF Energy Research [11] and previously documented [12–14]. The transport cost model relies on the pipeline cost model developed by Knoope et al. [15] and the storage cost model relies on the Zero Emission Platform for Zero Emission Fossil Fuel Power Plants [16].

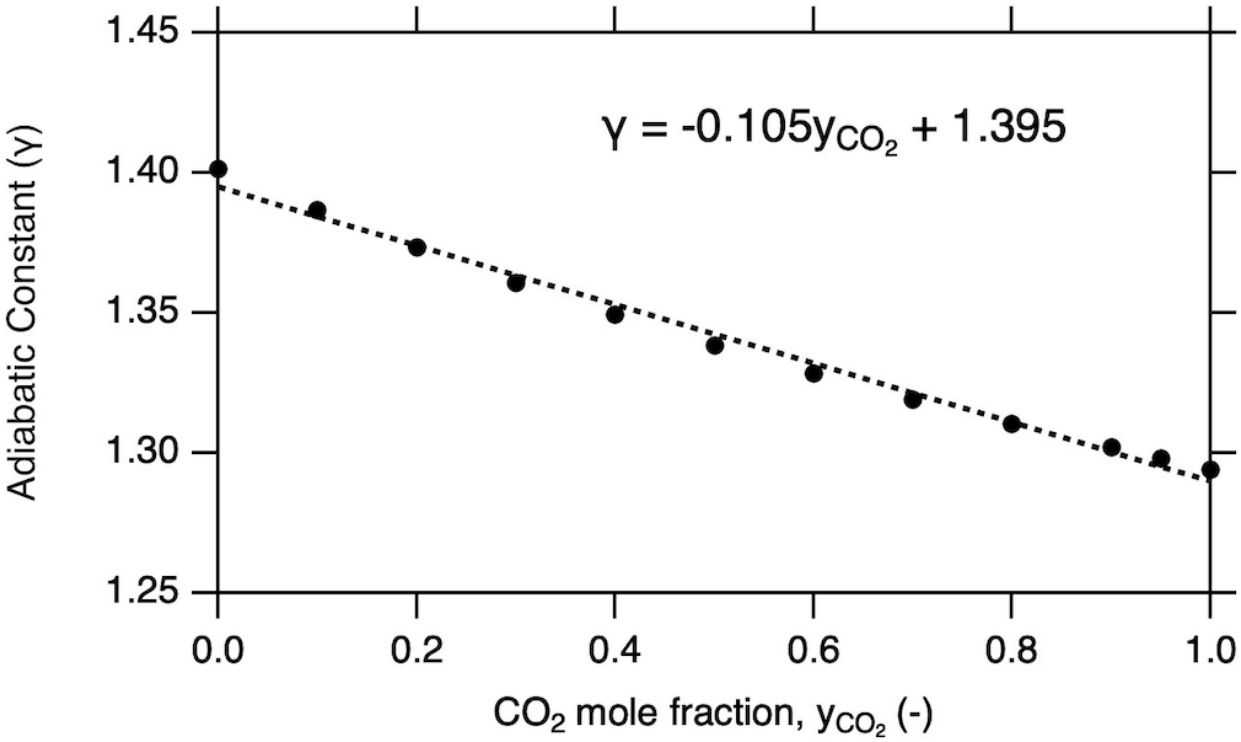

Figure S2: Linear dependence of adiabatic constant (γ) as a function of CO_2 mole fraction. Note that the γ values were obtained from NIST database [9].

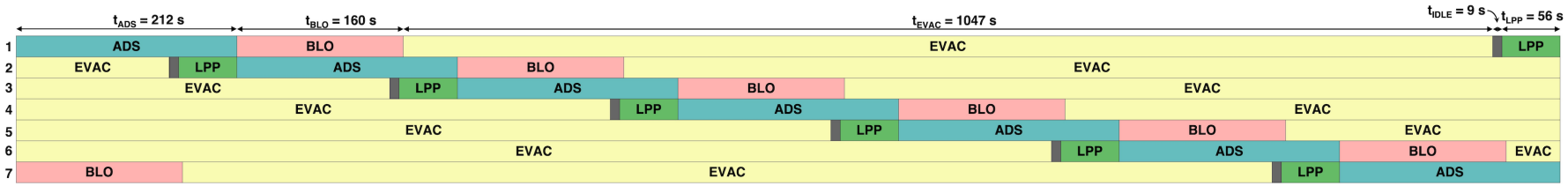

(a) Zeolite 13X

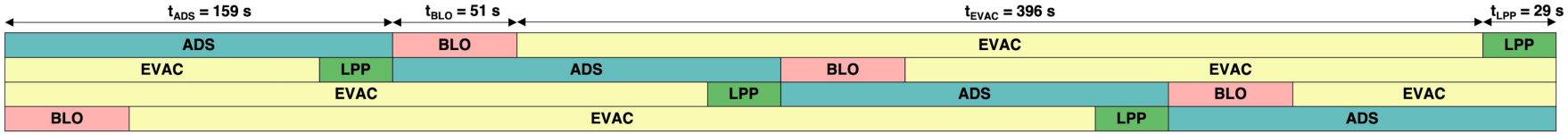

(b) UTSA-16

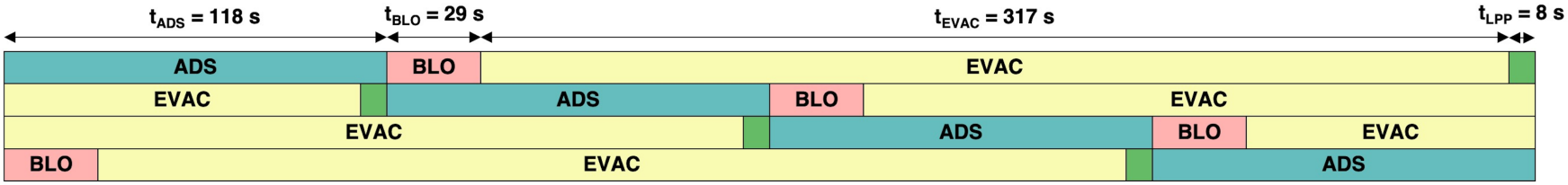

(c) IISERP MOF2

Figure S3: Optimal cycle schedules for all three adsorbents.

References

[1] IEAGHG, Techno-economic evaluation of SMR based standalone (merchant) plant with CCS, 2017/02. February 2017.

[2] Roussanaly, S.; Anantharaman, R.; Fu., C. Low-carbon footprint hydrogen production from natural gas: A techno-economic analysis of carbon capture and storage from steam-methane reforming. *Chem. Eng. Trans.* **2020** (Accepted).

[3] Haghpanah, R.; Majumder, A.; Nilam, R.; Rajendran, A.; Farooq, S.; Karimi, I. A.; Amanullah, M. Multiobjective optimization of a four-step adsorption process for postcombustion CO_2 capture via finite volume simulation. *Ind. Eng. Chem. Res* **2013**, *52*, 4249–4265.

[4] Agueda, V. I.; Delgado, J. A.; Uguina, M. A.; Brea, P.; Spjelkavik, A. I.; Blom, R.; Grande, C. Adsorption and diffusion of H_2, N_2, CO, CH_4 and CO_2 in UTSA-16 metal-organic framework extrudates. *Chem. Eng. Sci.* **2015**, *124*, 159 – 169.

[5] Burns, T. D.; Pai, K. N.; Subraveti, S. G.; Collins, S. P.; Krykunov, M.; Rajendran, A.; Woo, T. K. Prediction of MOF performance in vacuum swing adsorption systems for post-combustion CO_2 capture based on integrated molecular simulations, process optimizations, and machine learning models. *Environ. Sci. Technol.* **2020**, *54*, 4536–4544.

[6] Khurana, M.; Farooq, S. Integrated adsorbent process optimization for minimum cost of electricity including carbon capture by a VSA process. *AIChE J.* **2019**, *65*, 184–195.

[7] Susarla, N.; Haghpanah, R.; Karimi, I.; Farooq, S.; Rajendran, A.; Tan, L. S. C.; Lim, J. S. T. Energy and cost estimates for capturing CO_2 from a dry flue gas using pressure/vacuum swing adsorption. *Chem. Eng. Res. Des.* **2015**, *102*, 354 – 367.

[8] Roussanaly, S.; Anantharaman, R.; Lindqvist, K.; Hagen, B. A new approach to the identification of high-potential materials for cost-efficient membrane-based post-combustion CO_2 capture. *Sustain. Energy Fuels* **2018**, *2*, 1225–1243.

[9] Lemmon, E.; Huber, M.; McLinden, M. NIST standard reference database 23: Reference fluid thermodynamic and transport properties-REFPROP, Version 9.1. 2013.

[10] Deng, H.; Roussanaly, S.; Skaugen, G. Techno-economic analyses of CO_2 liquefaction: Impact of product pressure and impurities. *Int. J. Refrig.* **2019**, *103*, 301 – 315.

[11] Jakobsen, J.; Roussanaly, S.; Anantharaman, R. A techno-economic case study of CO_2 capture, transport and storage chain from a cement plant in Norway. *J. Clean. Prod.* **2017**, *144*, 523 – 539.

[12] Roussanaly, S.; Brunsvold, A. L.; Hognes, E. S. Benchmarking of CO_2 transport technologies: Part II – Offshore pipeline and shipping to an offshore site. *Int. J. Greenh. Gas Control* **2014**, *28*, 283 – 299.

[13] Roussanaly, S.; Grimstad, A.-A. The Economic value of CO_2 for EOR applications. *Energy Procedia* **2014**, *63*, 7836 – 7843.

[14] Skaugen, G.; Roussanaly, S.; Jakobsen, J.; Brunsvold, A. Techno-economic evaluation of the effects of impurities on conditioning and transport of CO_2 by pipeline. *Int. J. Greenh. Gas Control* **2016**, *54*, 627 – 639.

[15] Knoope, M.; Guijt, W.; Ramírez, A.; Faaij, A. Improved cost models for optimizing CO_2 pipeline configuration for point-to-point pipelines and simple networks. *Int. J. Greenh. Gas Control* **2014**, *22*, 25 – 46.

[16] European Technology Platform for Zero Emission Fossil Fuel Power Plants (ZEP), The costs of CO_2 storage, post-demonstration CCS in the EU, Brussels, Belgium. 2011.